SAND2007-1819C

Dynamics of Cable Harnesses on Large Precision Structures

Emil V. Ardelean[1]
Science Applications International Corporation, Albuquerque, New Mexico, 87106

James C. Goodding[2], Gregory Mehle,[3] and Douglas M. Coombs[4]
CSA Engineering, Albuquerque, New Mexico, 87123

Vít Babuška[5]
Sandia National Laboratories, Albuquerque, NM 87185

and

Lawrence M. Robertson, III,[6] Steven A. Lane,[7] Brea R. Ingram,[8] and Eric J. Hansen[9]
AFRL/VSSV, Kirtland AFB, New Mexico, 87117

This paper presents experimental results and modeling aspects for electrical power and signal cable harnesses used for space applications. Dynamics of large precision structures can be significantly influenced by subsystems such as electrical cables and harnesses as the structural mass of those structures tends to become smaller, and the quantity of attached cables continues to increase largely due to the ever increasing complexity of such structures. Contributions of cables to structural dynamic responses were observed but never studied, except for a low scale research effort conducted at the Air Force Research Laboratory, Space Vehicles Directorate (AFRL/VSSV). General observations were that at low frequencies cables have a mass loading effect while at higher frequencies they have a dissipative effect. The cables studied here adhere to space industry practices, identified through an extensive industry survey. Experimental procedures for extracting structural properties of the cables were developed. The structural properties of the cables extracted from the extensive experimental database that is being created can be used for numerical modeling of cabled structures. Explicit methods for analytical modeling of electrical cables attached to a structure in general are yet to be developed and the goal of this effort is to advance the state of the art in modeling cable harnesses mounted on lightweight spacecraft structures.

Nomenclature

A	=	cross section area
E	=	Young's modulus
I	=	area moment of inertia
L	=	cable length
M	=	beam/cable lineal mass
m	=	suspended mass

[1] Senior Mechanical Engineer, 2109 Air Park Road SE, AIAA Member
[2] Associate Principal Engineer, 1451 Innovation Parkway SE Suite 100, AIAA Member
[3] Senior Engineer, 1451 Innovation Parkway SE Suite 100, AIAA Member
[4] Engineer, 1451 Innovation Parkway SE Suite 100
[5] Principal Member of the Technical Staff, P.O. Box 5800 MS 0847, AIAA Associate Fellow
[6] Principal Aerospace Engineer, 3550 Aberdeen Ave. SE, AIAA Associate Fellow
[7] Senior Aerospace Engineer, 3550 Aberdeen Ave. SE, AIAA Senior Member
[8] 1st Lieutenant US Air Force, 3550 Aberdeen Ave SE
[9] Captain US Air Force, 3550 Aberdeen Ave. SE, AIAA Member (MB)

λ_n = beam frequency parameter for mode n
ω_n = circular natural frequency

I. Introduction

SPACE industry is striving to develop lightweight precision payload structures of ever increasing complexity and performance, and often deployable. The performance of these structures can be affected by a multitude of factors, one of them being the structural dynamics of the spacecraft. It is important, therefore, that accurate models are developed for structures that can not be fully tested on the ground. Accurate modeling is especially important for precision structures, like imaging systems, in order to reduce conservatism in the design phase and develop model based high performance controllers. In this context it was observed that the dynamic response of spacecraft in general can be significantly influenced by electrical power and signal cable harnesses. This is especially true for large precision structures. As the structural mass of large precision structures tends to become smaller the quantity of required electrical cables continues to increase largely due to the ever increasing complexity of such structures. An industry survey showed that in general cables mass accounts for 6-7% and in some cases for up to 15-20% of the total mass of the spacecraft. An illustrative example is presented in Figure 1. Therefore, the importance of understating the physical characteristics of the cables attached to these structures increases, since the behavior of precision structures can only be accurately modeled if their accompanied cables are also understood and modeled.

Figure 1. Electrical power and signal cables on a spacecraft.

Cables effects on various structures were observed but never extensively studied. General observations were that at low frequencies cables have a mass loading effect while at higher frequencies they have a dissipative effect. These observations were confirmed by an AFRL/VSSV research effort that attempted to quantify the effects of cables on simple structures such as a beam and a simple truss. Although insightful, the experimental results obtained through studying the cabled beam and truss raised more questions and a method for quantifying cables effects could not be established.[1]

Extensive research has been done in the past on wire rope and cable structures, however these well established results cannot be applied for the problem at hand due to the entirely different nature of the problem.[2,3] Explicit methods for analytical modeling of electrical cables attached to a structure in general are yet to be developed, current modeling techniques accounting only for non-structural mass loading of electrical cable harnesses. Although by using this approach the inertial properties of the spacecraft can be accurately predicted the structural dynamic models can grossly misrepresent the actual structure.

This paper presents experimental results and modeling aspects for a particular class of electrical power and signal cables harnesses used for space applications. To study all cable types that are used for space applications would be a next to impossible objective. Therefore, the scope of the endeavor was limited to a class of cables that was identified as the most commonly used in space applications. The cables studied adhere to space industry practices, identified through an extensive industry survey that revealed an abundance of cable types and configurations, fabrication and attachment procedures.

Work presented here is part of a larger effort investigating the effect of the cables on structural dynamics in general and structural dynamics of precision structures in particular. The described effort is to advance the state of the art in modeling cable harnesses mounted on lightweight spacecraft structures.

II. Motivation

A number of US Government laboratories are supporting research and development efforts to improve the accuracy and frequency bandwidth of test-verified structural dynamic modeling for complex, precision space structures. The impetus behind these efforts is the projection that future precision spacecraft may be too large and compliant to undergo system-level testing prior to launch. Without a system-level test, there will be increased reliance on performance prediction through modeling. A need to improve the capabilities for dynamic response predictions of precision structures, without large uncertainty factors, is needed. The dynamic effect introduced by cabling on precision space structures was identified as a significant issue at the 2005 Structural Vibrations Modeling and Validation (SVMV) forum.

In an attempt to respond to this need a low level research effort conducted at AFRL/VSSV between 2003 and 2004 aimed at developing a basic understanding of the effects of electrical cables on structural dynamics of host structures. Extensive literature research on the topic of electrical cables effects on structural dynamics was not fruitful, so it was considered that an experimental study was necessary in order to gain basic understanding of the dynamic interaction between cables and simple structures. A beam and a truss were used for the study, however, no guidelines from the space industry were followed. Cabling was done by using Teflon coated electrical wires, attached to the host structures with wire ties (zip-ties), as seen in Figure 2. Tests were conducted without cables and with various numbers of cables with different numbers of attachment points. The wires used for the experiments had a mass of 21g each.

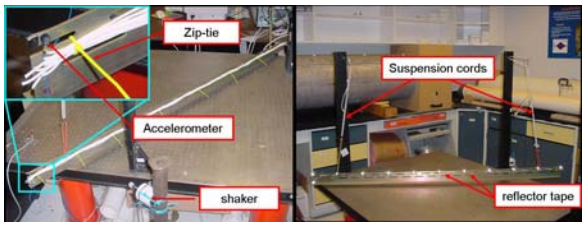

Figure 2. Experimental setup for quantifying cabling effects on a beam. *This experiment was designed to investigate the structural dynamics effects introduced by cables, however, it did not follow any space industry guidelines.*

The first set of tests was conducted on an aluminum alloy beam, presented in Figure 2. The beam was 1.78m (70in) long and weighted 3.3kg. It was suspended near the ends with bungee cords such that the rigid body modal frequencies were well separated from the structure's flexible modal frequencies. Frequency response functions (FRFs) were measured using two actuator and sensor experimental configurations: 1) an electro-dynamic shaker and laser vibrometer and 2) a modal impact hammer and accelerometer. For the sake of comparison, the results were almost identical. Typical FRFs between a collocated impact hammer and accelerometer for bare and cabled beam are like those presented in Figure 3.

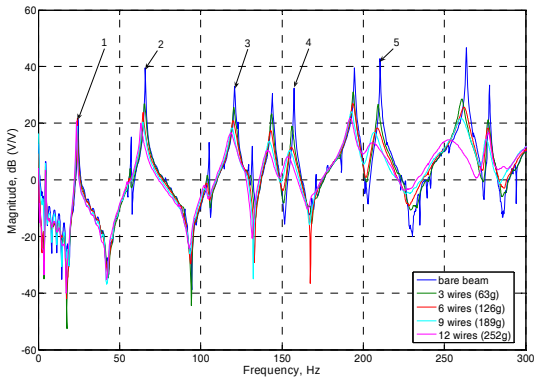

Figure 3. Collocated FRFs as a function of the number of wires attached to the beam. *First five bending modes of the beam are indicated by numbered arrows.*

It is evident in Figure 3 that cables increased the damping and caused variation in the modal frequency values, but the quantitative effect was mode order dependent. In general, the higher the cable-to-structure mass fraction, the more pronounced was the effect. The effect of the number of tie-down points appeared to be non-linear and small changes caused large variations in the response.

The effects of cables mounted on the beam had a high degree of consistency; all modes were affected in a fairly similar manner, however, the effects were more interesting and sometimes counterintuitive for the truss structure shown in Figure 4**Error! Reference source not found.**. The truss was built using four beams identical to the single beam previously described, and some connecting parts. In this case, all flexible modes of the structure in the frequency range of interest were taken into consideration. For the bare structure, COSMOS Works FEA results presented in Figure 4 are in very good agreement with experimental results. However, for the cabled truss, a FEA model that would capture the behavior of the truss with reasonable accuracy could not be developed. Figure 5 presents the collocated FRFs in two frequency bands in order to underline the difference between low frequency effects and high frequency effects (note that the terms low frequency and high frequency are relative). One can immediately observe that in the low frequency domain the cables introduce a mass loading effect and additional damping. However, in the high frequency domain a strong dissipation effect is the dominant,

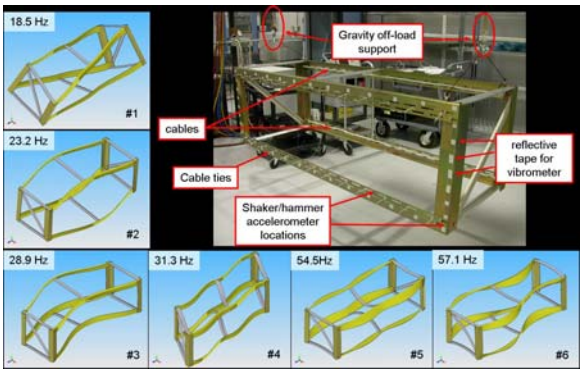

Figure 4. Experimental setup for the truss and CosmosWorks results for uncabled structure. *FEA results are in very good agreement with experimental data.*

although, less expected effects, like local increase in the response amplitude and increase of modal frequencies, are also present.

While a complete interpretation of the results obtained through these experiments is not intended here, one must observe the very strong dynamic interaction between cables/wires and host structures even when their mass ratio was relatively small. Along with the feedback received from industry regarding the effects introduced by electrical cable harnesses, this research motivated a new and more systematic approach to this problem.

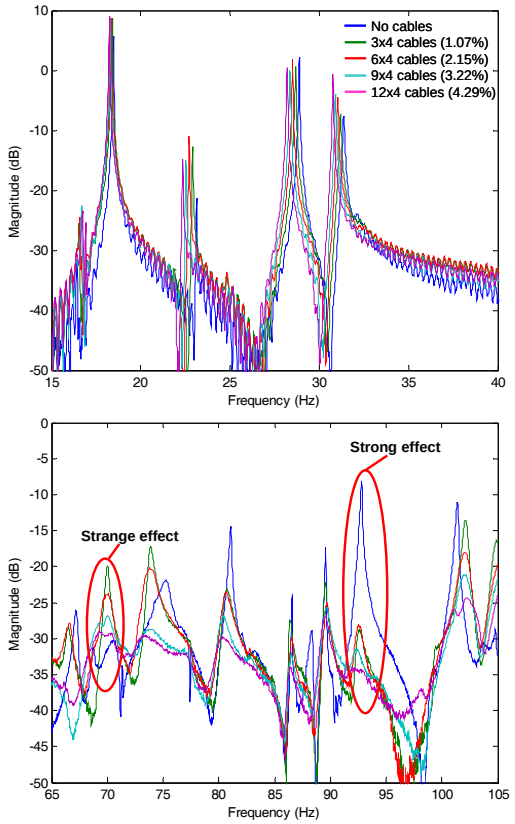

Figure 5. Collocated FRFs for the truss. *Results are presented in two frequency bands in order to underline the difference between low frequency effects and high frequency effects.*

III. General Considerations

Accurate structural modeling of spacecraft implies a good understanding of the physics that governs the dynamics of the individual components. As mentioned above the amount of electrical cable harnesses relative to the total mass of spacecraft becomes more and more significant. Hence, it is important to understand the dynamics of the cable harnesses alone before trying to understand their effects on complex structures.

A. Industry Survey

The research effort presented here began with an extensive industry survey to understand the state of the art in electrical wiring of spacecraft.[1] It was discovered that wiring is done according to various guides and standards, however, no all inclusive standard exists regarding this topic.[4,5,6,7] Extensive discussions with integration personnel at AFRL revealed that cabling a spacecraft is a kind of an art form. Since spacecraft are usually unique a wide variety of cable harnesses and attachment methods exist, and what it is actually done on the spacecraft is somewhat a matter of trade and experience. Therefore, a first task for this study was to identify the most common cables and attachment methods used for space applications. It was found that cables used for space applications are made of MIL spec, Teflon coated wires of size ranging from 20 AWG (American Wire Gauge) to 30 AWG, normally in twisted pairs then stitched and wrapped together to form a harness.[4] The cable harnesses are then attached to the host structure through mounting plates and secured in place with cable ties (zip-ties) or lacing chord/tape, as shown in Figure 6. Cable's attachment to a structure.

B. Trade Space

To study all types of space qualified cables and attachment methods was unfeasible, therefore, the trade space was limited to the most representative classes. Electrical wires used for experiments were in conformity with MIL-W-22759/12 (formerly MS 21986) consisting of nickel plated copper with Teflon insulation 0.010 inches (0.254mm) thick, rated for a temperature of 260ºC and a voltage of 600V (see Figure7**Error! Reference source not found.**).

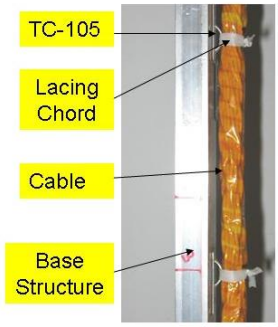

Figure 6. Cable's attachment to a structure

To form a cable the wires were twisted in pairs (to cancel the electro-magnetic field) and then stitched with lacing chord according to NASA-STD-8739.4, Chapter 9. There is no recommendation regarding the pitch of the twist for the twisted pairs, however a pitch equal to approx.

ten times the wire diameter is a good value. The standard shows, however, how to do the stitching and gives recommendations for the distance between ties as a function of the harness diameter. After stitching the wires are wrapped in Kapton with about 50% overlap. Figure 8 shows the fabrication procedure and several samples having different numbers of twisted pairs and different wire diameters.

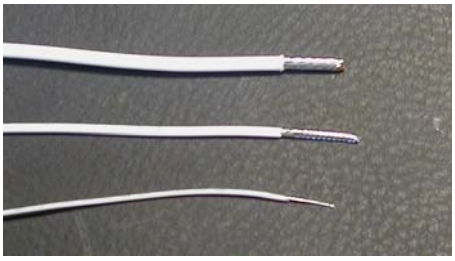

Figure7. MIL spec electrical wires used for testing.

Figure 8. Fabrication of cables for space applications. *Twisted conductor pairs are stitched together with lacing chord then wrapped with Kapton tape. Samples consisting of different numbers of conductors and conductor gauges are shown.*

A cable fabricated as described is a composite-like structure. Since it is difficult to analytically model its dynamic behavior, an experiment-to-model approach was considered the most appropriate. The dynamics of a cable of interest in this research is potentially influenced by any of its parameters: wire size and twist, number of wires in the bundle, stitching, nature and tightness of wrapping. In order to determine the influence of each of these parameters and obtain representative characteristics of cables, two classes of tests were employed, namely, lateral, and axial tests. Lateral tests represent the bulk of the experimental work since one could easily tell that cables attached to a vibrating structure are exercised primarily in bending. Axial tests were deemed necessary to complement lateral tests in order to determine an effective Young's modulus for cable as a whole, as described in Section IV. A.

An important factor that must be taken into account is the excitation levels for lateral testing. Of interest are the effects that cables introduce on large precision structures during normal operation, which takes place in a "zero g" environment. Therefore, excitation levels consistent with those must be used for experimental investigations. However, for the sake of completeness of the study, excitation levels well above those encountered in space were also used during experiments. Taking into consideration all of the above mentioned variables a large test matrix was conceived. The test matrix is being filled in and will form the foundation of a handbook and design guide to serve the spacecraft designer.

IV. Dynamics of Cables

Fundamental conductor and harness properties are obvious necessities for building appropriate models of harnesses to predict their influence on space structure dynamics. Information on cable's physical dimensions and mass is readily available through direct measurements. However, other parameters have to be determined through experimental investigations. Determination of those parameters, namely, geometrical moment of inertia, I, Young's modulus, E, shear modulus, G, etc., is a convoluted process due to the composite-like nature of the cables. However, it is possible to extract these parameters through relatively simple tests. To that end, test methods, techniques and rigs were devised to generate experimental databases for property estimation.

A. Conductor and Cable Axial Test Methods and Results

Cable tensile stiffness properties were determined using a resonant test method by suspending a mass on a free end of the test article. The test rig is shown in

Figure 9 along with a detail showing the instrumentation used.

The test method is based on measuring the driving point inertance at the test specimen free end using an instrumented impact hammer and accelerometer. These driving point inertance FRFs are dominated by the "plunge mode" that is analogous of a single degree of freedom system. Achieving a driving point along the test article centerline was important to minimize exciting end mass "rocking modes" or test article "string modes."

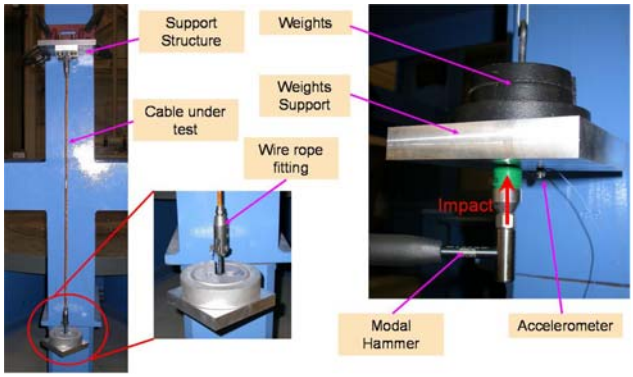

Figure 9. Experimental setup for dynamic axial testing.

The objective of these tests was to determine estimates of extensional modulus at zero suspended load, as would be expected for a harness in service. Driving point inertance FRFs were acquired for the specimen under test with different suspended masses to determine the sensitivity of extensional modulus to the applied load. This test series also studied Young's Modulus for "parallel conductor" and cable construction types. Parallel conductor test specimens were fabricated by laying single conductor wires side-by-side to make up an assembly without helical twisting, as was done for the cable harness test specimens. The test articles used in this test series included the following.

- Parallel conductors
  - 20 AWG; 1, 2 and 4 conductors
  - 22 AWG; 1, 2 and 4 conductors
  - 24 AWG; 1, 2 and 4 conductors
  - 26 AWG; 1, 2 and 4 conductors
- Cable harnesses
  - 22 AWG, 7 twisted pairs
  - 26 AWG, 7 twisted pairs

The assumed model is of a rod in tension that follows Hooke's law. The value of cross sectional area was assumed to be the total cross sectional area of copper conductor in from MIL-STD wire catalog values. The expression for Young's Modulus, assuming that the cable behaves as a massless tensile member with a point mass at its free end, is given in Equation 1.

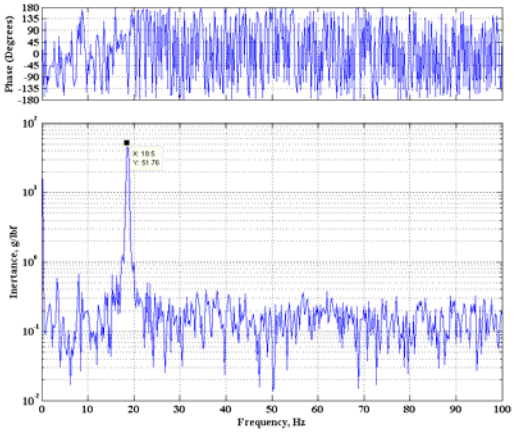

Figure 10. Driving point inertance FRF

$$E = \frac{\omega_n^{\,2} mL}{A} \tag{1}$$

Figure 10 shows a typical driving point inertance FRF from this test series. The elevated noise floor is due to the low response level and the relatively high accelerometer noise floor. This does not, however, affect the identification of the plunge mode resonant frequency, because at resonance, the signal is 40 dB above the noise floor. Resonant frequencies for test articles suspending different end masses were tabulated and processed to estimate Young's Modulus.

A plot showing the estimated Young's Modulus as a function of the applied load per conductor for 26 AWG wire appears in Figure 11. While the low number of samples in the measurement set limits an estimate of error bars, it is clear that the modulus increases with increasing load per conductor. The cause of the increasing modulus as a function of tensile load per conductor is being researched; the appropriateness of a linear fit to extrapolate to zero tensile load is unclear. Assuming a linear relationship between modulus and load per conductor, the apparent Young's modulus at zero tensile load is roughly 70 percent of copper's, for the straight conductor test specimens.

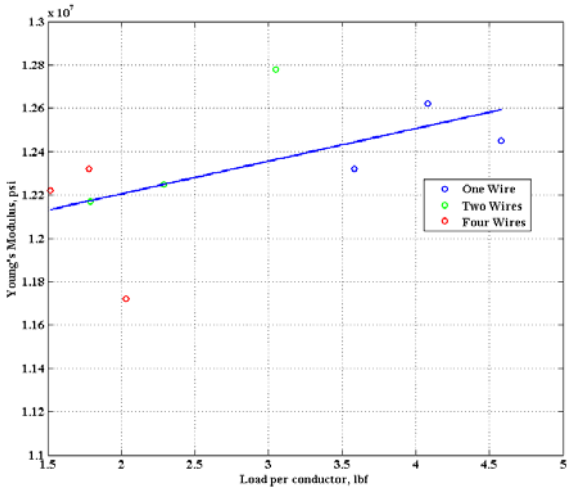

Figure 11. Young's Modulus as a function of load.

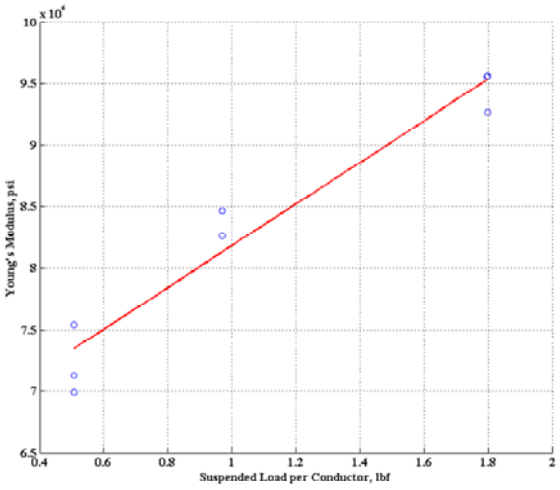

Figure 12. Harness Young's modulus as function of load

Figure 12 depicts results from 26 AWG harness measurements. This figure shows that the apparent modulus is more sensitive to tensile load than are individual conductors, but it should be noted that the load-per-conductor in the harness measurements are lower than in the straight conductor tests. This may be an indication that a linear function is not appropriate at light tensile loads. With the assumption that the relation is linear, the effective modulus is approximately 38 percent of that of copper. Compensation for harness construction is being researched.

B. Cable Lateral Test

1. Experimental Setup and Data Aquisition

Lateral motion, or bending, was identified as the main type of motion that cables experience on the vibrating base structure. Although the cables of interest in this study exhibit a beam-like behavior, as shown in the following, experimental testing of cables alone proved itself to be a tricky affair.

In a normal beam test one can choose between modal hammer and shakers to produce excitation. Using a modal hammer for lateral excitation of cables would be very unpractical; therefore, one is limited to using a shaker. Furthermore, the load cell cannot be easily attached to the cable for obvious reasons. Placing a regular stinger between the load cell and the cable under test would result in corrupt FRFs; stinger modes would be present along with cable modes. Hence, a connector, showed in Figure 13, was designed. The connector, allows the cable to bend freely, and transmits the imparted load to the specimen under test without adding parasitic dynamics.

High sensitivity of the instruments used for lateral testing was of great importance since numerous cable samples that were tested are highly flexible and light. A PCB miniature load cell with sensitivity of 526.8mV/N was used to measure the input forcing, and a Polytec laser vibrometer with a sensitivity of 125mm/s/V was used to measure the output cable velocity.

Another important aspect regarding lateral testing were the boundary conditions (BCs). Because of the cable's flexibility it is almost impossible to emulate free-free BCs. A number of samples exhibit a first flexible mode below 5Hz, therefore, their FRFs were corrupted by the dynamics of the strings used for cable's support. The experimental setup illustrated in Figure 13 facilitated testing of cables of various dimensions and with three types of BCs, namely pinned, using TC-105 tabs and zip-ties, and clamped. The pinned and clamped BCs were used both for the sake of model validation, while the TC-105/zip-tie BC was used for evaluating the parameters for realistic conditions.

All tests were conducted using band-limited random excitation generated with a SigLab system, and data was collected using SigLab and Polytec Scanning Vibrometer. The bulk of experiments conducted to characterize the dynamic behavior of cables, involved excitation in the range of 10mg to 100mg (0.098–0.98m/s^2). These levels are still well above those normally encountered by a structure on orbit, but the lowest level was dictated by the sensitivity of instrumentation.

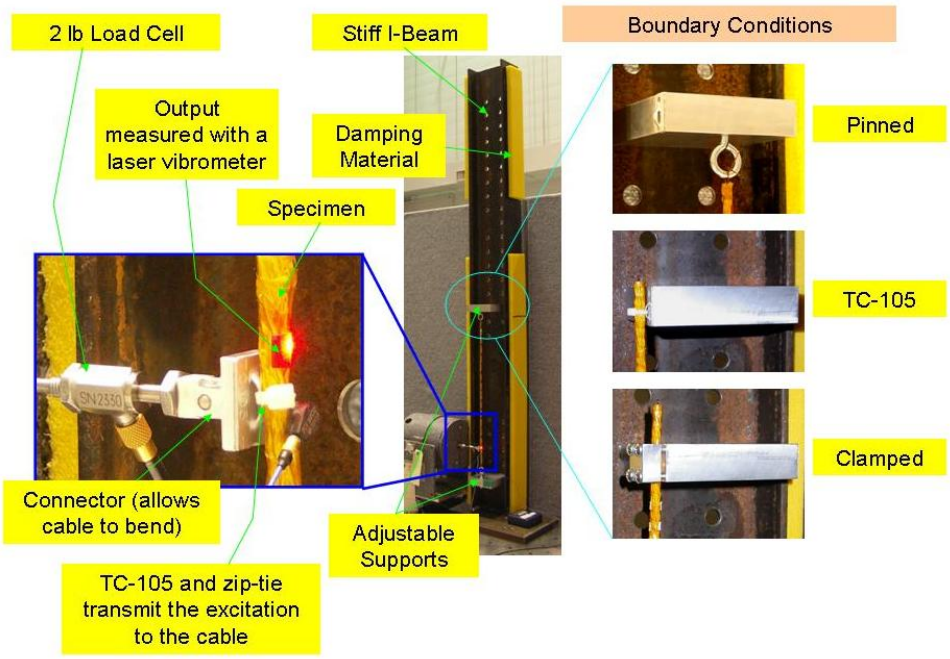

Figure 13. Experimental setup for lateral testing.

Figure 14 presents a set of typical mobility FRF obtained for sample 26-10-7 (26 AWG, 10 twisted pairs, sample # 7) with different excitation levels. As mentioned above the lowest excitation level pushed the load cell's sensitivity threshold indicated by reduced coherence below 2Hz. Interestingly enough, cables exhibited a behavior independent of driving amplitude for driving levels below 50mg, as one can see in Figure 15. As shown in the following the modal frequency progression for all studied cables follows a quadratic relationship, like a Bernoulli-Euler beam, however, a Bernoulli-Euler beam model cannot completely describe a cable's structural dynamic behavior.

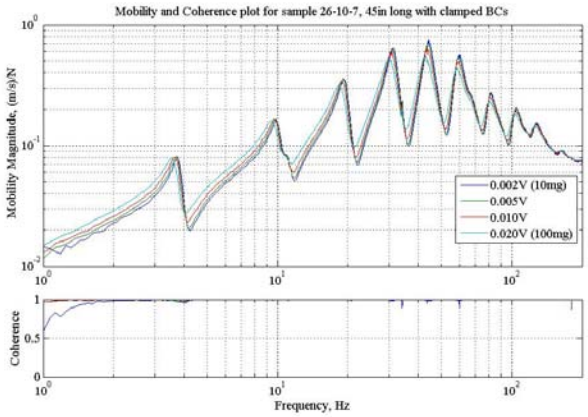

Figure 14. Mobility FRF for a 26 AWG, 10 pair (26-10-7), 45-inches long, with clamped BCs.

objectives included estimating effective mass, natural frequency and damping ratio at each resonance. These parameters formed the database used to study the underlying relationships between cable harness construction (i.e., conductor gauge, twisted pair count and length) and its dynamics. Developing well defined relationships, either

2. Signal Processing Method

The study of cable dynamics when subjected to lateral dynamic loading was based on standard curve fitting techniques for modal analysis of linear structures. The signal processing

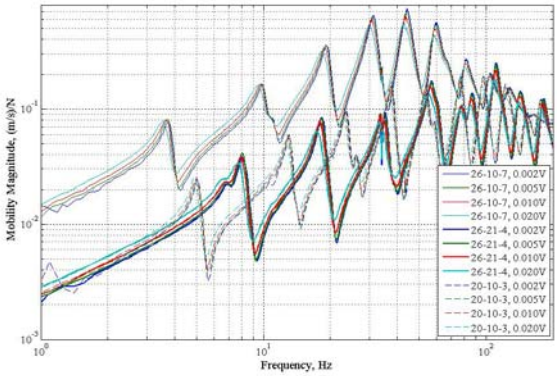

Figure 15. Mobility FRF for different samples 45-inches long, with clamped BCs. *Samples behave nearly linearly for excitation levels not exceeding 50mg.*

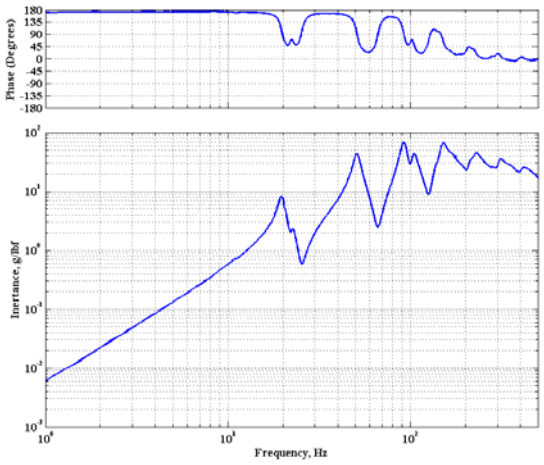

Figure 16. Cable inertance FRF.

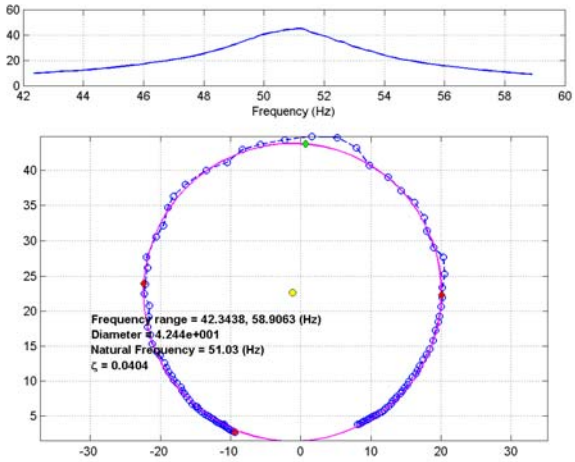

Figure 17. Circle fit display.

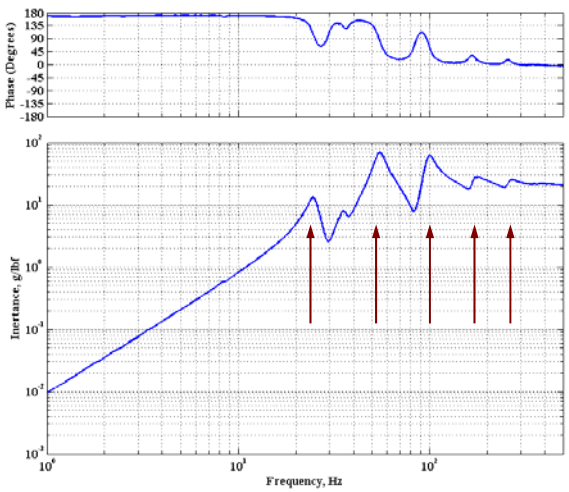

Figure 18. Inertance FRF and natural frequency spacing.

empirical or analytical, form the foundation for the cable effects applied research.

A circle fitting algorithm was selected for its ease of use, and extensive user interaction; it is a so-called single degree of freedom fitter, which works well if the modes are well separated and relatively lightly damped. Each mobility frequency response function measured in the laboratory was scaled to be in engineering units. The inertance function was then computed from the mobility FRF as the initial step for signal processing. Figure 16 depicts an example inertance FRF from the lateral test series. The low frequency asymptote, with the 40 dB per decade slope, is identical to that of a spring to ground. The regular spacing of the cable resonances and high signal-to-noise ratio is apparent in this driving point FRF. This figure does illustrate the influence of "fixture modes" on the measurement, particularly at the first and third modes.

Figure 17 depicts a circle fit. The upper subplot shows the FRF magnitude component; the lower subplot shows the measurement (with a blue circle and line segments) and the least squares best fit circle to the data with a solid magenta line texture. The resonant frequency and half power points are denoted by green and red diamonds respectively. As noted earlier, fixture modes couple into cable modes and complicate the curve fitting process. To reduce the influence of these spurious modes, the curve fitting algorithm was customized to determine if any outliers exist within the curve fitting range frequency range. If the radius from the circle center to any data point exceeds 3.5 standard deviations, the user is prompted to select a frequency range where a Satvitzky-Golay polynomial filter is applied. While this technique requires user interaction and engineering judgment, it has been shown to provide good modal parameter estimates, even with the presence of fixture modes strongly coupled to cable dynamics.

3. Modal Parameter Results

Analysis of the lateral cable harness dynamic test results illustrated a fundamental property of twisted pair, stitched and Kapton wrapped construction: the natural frequencies follow a unique (and deterministic) progression law. The implication of this finding is that low frequency cable harness dynamics (as constructed and tested) may be modeled with standard techniques. Figure 18 depicts an inertance frequency response function from a 26 AWG cable harness sample, with arrows highlighting the system natural frequencies. A plot of the natural frequencies, normalized by the first modal frequency is shown in Figure 19. Included on the axes in this figure is the quadratic least squares best fit to the five data points. This quadratic character in the natural frequency progression is observed for all of the harness types included in the lateral cable test series; the coefficients of the best fit second order polynomial have been shown to depend on cable construction details (i.e., twisted pair count and conductor

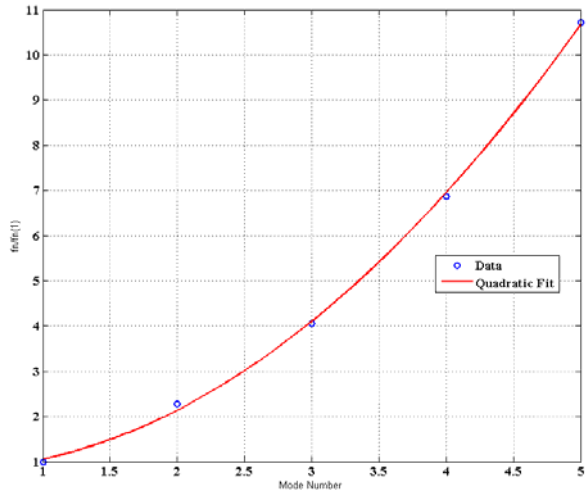

Figure 19. Normalized natural frequency progression.

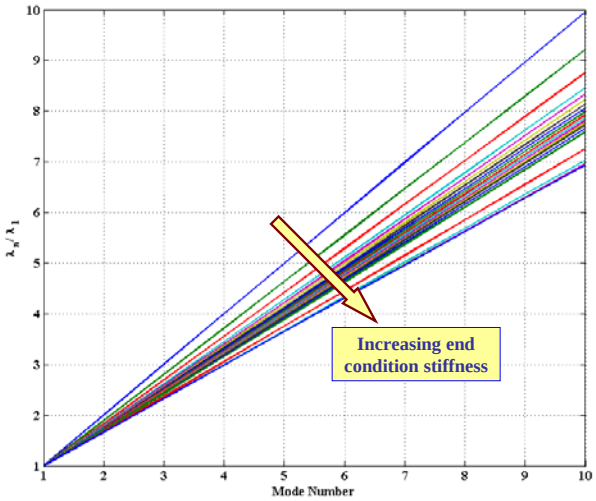

Figure 20. Beam frequency parameter ratio varying end condition stiffness.

gauge).

An Euler beam follows a similar natural frequency progression quadratic relationship. A finite element-based study was conducted using a simple Euler beam model, investigating the effect of torsional stiffness at the beam connection points to determine if a cable harness could be modeled as a beam with sprung boundary conditions at the connection points. The study estimated natural frequencies over a span of torsional spring rates normalized to the beam flexural stiffness. The beam natural frequency expression appears in equation 2; λ_n is the so-called frequency parameter and is a function of the boundary conditions. The finite element model results presented in Figure 20 are the square root of the predicted natural frequencies divided by the fundamental natural frequency for the non-dimensional stiffness at the support spanning from 0 (i.e., pure pinned-pinned condition) to 1,000 (i.e., approaching the clamped-clamped case). In the ideal pinned-pinned condition, the slope of the frequency parameter ratio versus mode number is unity; the slope decreases as the end condition stiffness increases, as shown in this figure. For a built-in beam (i.e., clamped-clamped conditions), the frequency parameter ratio slope is 0.67.

$$\omega_n = \frac{\lambda_n^2}{L^2}\sqrt{\frac{EI}{M}} \qquad \textbf{(2)}$$

Lateral harness experiments have shown that the while the frequency progression follows a quadratic relation to mode number, the slope of the normalized frequency parameter approaches one half. This indicates that a simple Euler beam model is not precise and research is underway to determine the appropriate model formulations to predict harness dynamics.

The data collected in these experiments was used to define *E*, *I*, *A*, and ρ (mass density) for the cables. These parameter values are being validated on a free-free beam. A discussion of this effort is given in Ref. 8.

Summary

As the space industry has matured, spacecraft have become more lightweight, include sensor packages of ever-increasing complexity while the requirements on mechanical stability to meet mission goals are becoming more demanding. As has been seen, but not studied previously, the effects of electrical harnesses on spacecraft can have a major impact on precision space structures that is not captured through standard modeling techniques. The experimental sequence to study the structural dynamic behavior of unsupported cable harnesses described in this paper is part of a research program that is advancing the state of the art for structural modeling for spacecraft. The scope of this research was restricted to a class of cables and cable harnesses that were identified as commonly used for space applications. Fabrication of cable samples used in the study followed industry standards. Experimental procedures that permit determination of physical properties of cables were developed and a large test matrix is currently being filled. Test results show that a cable harness, built following spacecraft integration standards does exhibit "beam-like" behavior. However, it was found that cable's dynamic behavior cannot be described with classical Bernoulli-Euler or Timoshenko beam models. Modeling techniques are being researched to predict the

harness dynamic characteristics and a handbook and design guide to serve the spacecraft designer is being developed.

Acknowledgments

The authors would like to thank the Air Force Office of Scientific Research and the Secretary of the Air Force government sponsor of this work. The authors would also like to thank the many industry, government and academic groups that responded to the initial survey of structural dynamic cable effects.

A portion of this work was performed at Sandia National Laboratories. Sandia is a multi-program laboratory operated by Sandia Corporation, a Lockheed Martin Company, for the United States Department of Energy's National Nuclear Security Administration under contract DE-AC04-94AL85000.

References

[1]Lawrence M. "Robbie" Robertson, et al, "Cable Effects on the Dynamics of Large Precision Structures", *AIAA SDM conference*, Hawaii, April 2007.

[2]George A. Costello, *Theory of Wire Rope*, Springer-Verlag, New York, 1990.

[3]H. Max Irvine (ed), *Cable Structures*, The MIT Press, Cambridge, Massachusetts, 1981.

[4]NASA-STD-8739.4, Crimping, Interconnecting Cables, Harnesses, and Wiring, February 1998.

[5]SAE-AS50881B, Wiring Aerospace Vehicles.

[6]MIL-HDBK-83575, General Handbook for Space Wiring Harness Design and Testing.

[7]ESA-CR(P)-1086, Guidelines for Spacecraft Power and Signal Cabling.

[8]James C. Goodding, et.al., "Study of Free-Free Beam Structural Dynamics Perturbations due to Mounted Cable Harnesses", *AIAA SDM conference*, Hawaii, April 2007.